Blockade of Insect Odorant Receptor Currents by Amiloride Derivatives

Gregory M. Pask[1], Yuriy V. Bobkov[2], Elizabeth A. Corey[2], Barry W. Ache[2,3] and Laurence J. Zwiebel[1,4]

[1]Department of Biological Sciences, Vanderbilt University, Nashville, Tennessee, [2]Whitney Laboratory, Center for Smell and Taste, and McKnight Brain Institute, University of Florida, Gainesville, Florida, [3]Departments of Biology and Neuroscience, University of Florida, Gainesville, Florida and [4]Department of Pharmacology, Vanderbilt Brain Institute and Center for Human Genetics, Institutes of Chemical Biology and Global Health and Program in Developmental Biology, Vanderbilt University Medical Center, Nashville, Tennessee

Correspondence to be sent to: Laurence J. Zwiebel, Department of Biological Sciences, Vanderbilt University, Nashville, USA. email: l.zwiebel@vanderbilt.edu

Abstract

Insect odorant receptors (ORs) function as heteromeric odorant-gated ion channels consisting of a conserved coreceptor, Orco, and an odorant-sensitive tuning subunit. Although some OR modulators have been identified, an extended library of pharmacological tools is currently lacking and would aid in furthering our understanding of insect OR complexes. We now demonstrate that amiloride and several derivatives, which have been extensively used as blockers for various ion channels and transporters, also block odorant-gated currents from 2 OR complexes from the malaria vector mosquito *Anopheles gambiae*. In addition, both heteromeric and homomeric ORs were susceptible to amiloride blockade when activated by VUAA1, an agonist that targets the Orco channel subunit. Amiloride derivatives therefore represent a valuable class of channel blockers that can be used to investigate the pharmacological and biophysical properties of insect OR function.

Key words: amiloride, channel blocker, insect, odorant receptor

Introduction

Odorant receptors (ORs) are one of the principal chemosensory receptor families in insects and are responsible for detecting a wide range of volatile semiochemicals in the environment (Kaupp 2010). Housed within chemosensory sensilla on the olfactory organs, ORs on the dendrites of olfactory receptor neurons (ORNs) interact with odorant ligands, resulting in a depolarization that ultimately reaches the corresponding glomerulus in the antennal lobe. Insect ORs are 7-transmembrane proteins, with an inverted topology relative to G-protein-coupled receptors, and function as heteromeric odorant-gated cation channels (Benton et al. 2006; Lundin et al. 2007; Sato et al. 2008; Smart et al. 2008; Wicher et al. 2008; Jones et al. 2011). The role of metabotropic pathways in either direct or indirect modification of insect OR function is still unclear (Kaupp, 2010). An OR complex contains 2 types of subunits in an undetermined stoichiometry, an odorant-specific OR and the conserved coreceptor, Orco.

The recent discovery of an Orco family agonist, VUAA1, has provided insight into insect OR structure and function (Jones et al. 2011). When expressed alone, Orco subunits from several insect species can form functional homomeric channels, susceptible to activation by VUAA1 (Jones et al. 2011). In addition, differences in the pore-specific properties between several heteromeric OR complexes suggest that the odorant-specific OR contributes to the pore structure (Nichols et al. 2011; Pask et al. 2011; Nakagawa et al. 2012). Further examination of the structure–activity relationship of VUAA1 has yielded several more potent Orco agonists, as well as antagonists capable of reducing both VUAA1- and odorant-evoked currents through competitive and noncompetitive mechanisms, respectively (Chen and Luetje 2012; Jones et al. 2012). The identification of new insect OR modulators will provide additional pharmacological tools that can be useful in continuing to advance our understanding of the insect olfactory system.

To block insect OR responses, previous studies have utilized ruthenium red, a nonspecific blocker of numerous cation channels (Nakagawa et al. 2005; Sato et al. 2008; Jones et al. 2011; Nichols et al. 2011; Pask et al. 2011). The identification of other channel blockers with greater selectivity than ruthenium red would provide useful probes for the study of insect OR function. One candidate group of agents consists of amiloride and several related analogs, which have been shown to block epithelial sodium channels (ENaCs), acid-sensing ion channels, and Na^+/H^+ exchangers (Kleyman and Cragoe 1988; Frings et al. 1992; Ugawa et al. 2002). In arthropod olfactory systems, amiloride and its derivatives have been studied extensively in the lobster where they reversibly inhibit odorant-evoked activity (Bobkov and Ache 2007), and more recently amiloride has been shown to block *Drosophila melanogaster* chemosensory ionotropic receptors (Abuin et al. 2011).

Therefore, we have explored the ability of a panel of amilorides to block currents of 2 heteromeric OR channels from *An. gambiae*, as well as homomeric Orco channels from 4 insect orders. We demonstrate that insect ORs display varying degrees of susceptibility to channel blockade by amiloride derivatives, and we propose their use in pharmacological studies of insect OR function.

Materials and methods

Chemicals

The odorants, δ-decalactone (CAS 705-86-2) and eugenol (CAS 97-53-0), were purchased from Sigma–Aldrich. VUAA1 (N-(4-ethylphenyl)-2-((4-ethyl-5-(3-pyridinyl)-4H-1,2,4- triazol-3-yl)thio)acetamide) was purchased from ChemBridge corporation (ID# 7116565). The following amiloride derivatives were ordered from Sigma–Aldrich: Amiloride hydrochloride hydrate (**Amiloride**), CAS 2016-88-8; 5-(*N,N*-Dimethyl)amiloride hydrochloride (**DMA**), CAS 1214-79-5; 5-(N-Ethyl-N-isopropyl)amiloride (**EIPA**), CAS 1154-25-2; 5-(N-Methyl-N-isobutyl)amiloride (**MIA**), CAS 96861-65-3; 5-(N,N-Hexamethylene)amiloride (**HMA**), 1428-95-1; Phenamil methanesulfonate salt (**Phenamil**), CAS 1161-94-0; and 3',4'-Dichlorobenzamil hydrochloride (**DCBA**), CAS 1166-01-4. All of the above compounds were initially dissolved in dimethylsulfoxide (DMSO) and subsequently diluted in extracellular solution at a final concentration of 0.2% DMSO.

Cell culture and patch clamp electrophysiology

The generation and use of OR-expressing cell lines have been previously described (Bohbot et al. 2011). Cells were incubated with 0.3 μg/mL tetracycline for 16–24 h before the assay to induce OR expression.

Whole-cell patch clamp recordings were measured using an Axopatch 200B amplifier (Molecular Devices) and a Digidata 1322A (Molecular Devices) with a sampling rate of 10 kHz and low-pass filtered at 5 kHz. Holding potentials were between −60 and −50 mV, and all compound solutions were applied under continuous focal perfusion with either a Perfusion Pencil (Automate Scientific) or an RSC-160 rapid solution changer (Bio-Logic Science Instruments). Extracellular solutions contained (in mM) 140 NaCl; 1 $CaCl_2$; 0–1 $MgCl_2$; 5 KCl; 10 HEPES (Extracellular 1) or 130 NaCl, 34 glucose, 10 HEPES, 1.5 $CaCl_2$, 1.3 KH_2PO_4, 0.5 $MgSO_4$ (Extracellular 2) and the internal solutions contained either 140 NaCl; 1–2 EGTA; 10 HEPES (Internal 1) or 120 KCl, 30 glucose, 10 HEPES, 2 $MgCl_2$, 1.1 EGTA, 0.1 $CaCl_2$ (Internal 2). All solutions had a pH 7.35–7.4 and were adjusted with either Trizma-base (Sigma) or NaOH.

Data analysis

Current recordings were analyzed in pCLAMP 10 (Molecular Devices) and inhibition curves were generated with Prism 4 (Graphpad). Curves were fit with a sigmoidal dose–response (variable slope) Hill equation with 1.0 set as the top curve constraint. An analysis of variation (ANOVA) with a Bonferroni post test were used for all IC_{50} and histogram comparisons and were performed in Prism 4 (Graphpad).

Results

Whole-cell patch clamp assays were performed to test the effect of a panel of amilorides on *An. gambiae* ORs (AgOrs) heterologously expressed in human embryonic kidney (HEK) cells. The panel of derivatives consisted of amiloride, as well as amiloride analogs with varying substituents at the 5 position of the pyrazine ring and the terminal nitrogen of the guanidinium group (Figure 1). This panel was tested against cells expressing either AgOr48, a lactone receptor, or AgOr65, which is sensitive to eugenol, each coexpressed with AgOrco (Pask et al. 2013; Wang et al. 2010). Increasing concentrations of amiloride derivative were applied once agonist-induced currents reached a steady-state level.

During the application of a strong agonist, δ-decalactone, each of the amiloride derivatives caused substantial concentration-dependent blockade of odorant-evoked currents from AgOr48-expressing cells (Figure 2). Of these, amiloride was the least potent, with all structural modifications resulting in more potent blockade. The potency sequence for AgOr48 + AgOrco is HMA ~ MIA > EIPA > DMA ~ DCBA > Phenamil > Amiloride (see online supplementary Table S1 for IC_{50} values). The effects of many of the amiloride analogs were partially irreversible at high concentrations, as indicated by the observation that current amplitudes after wash-out of the blocker did not return to their initial levels. This decrease was not the result of constant agonist application as δ-decalactone-evoked currents reached a steady state and did not decrease over time (see online supplementary Figure S1). Overall, HMA
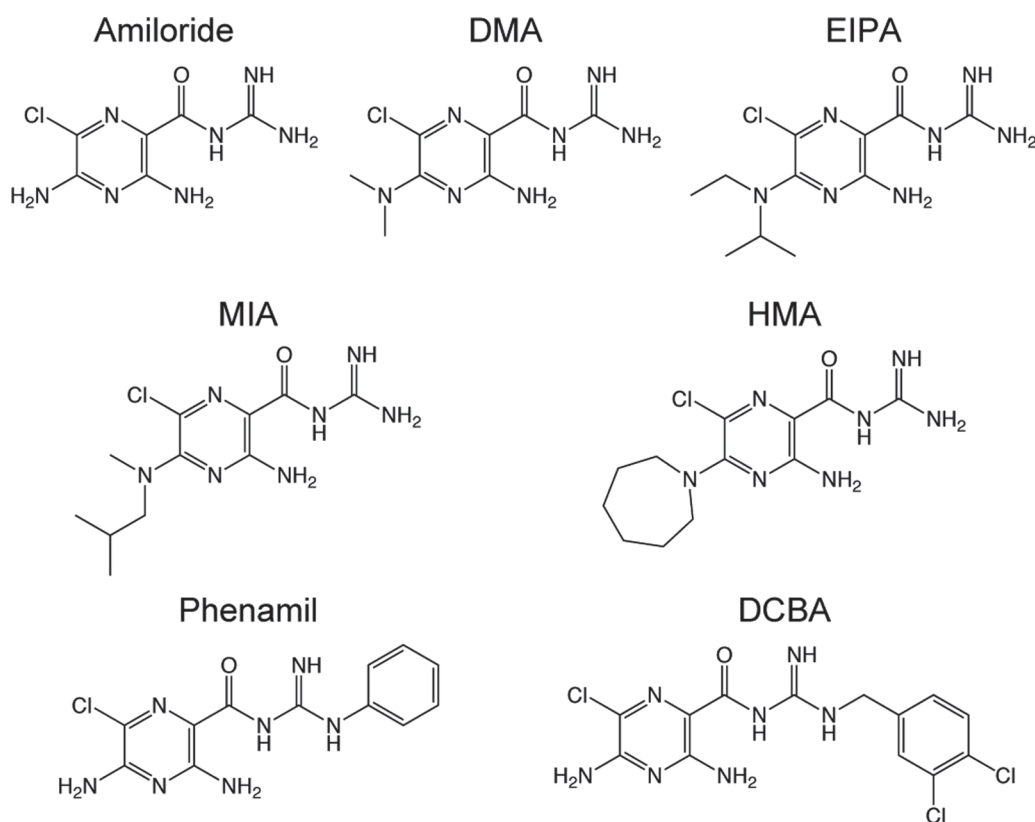
Figure 1 Chemical structures and abbreviations of the amiloride derivatives involved in this study.

(IC$_{50}$ = −5.05±0.02 logM) and MIA (IC$_{50}$ = −4.98±0.02 logM) were found to be the most potent channel blockers of the AgOr48 + AgOrco complex.

When the same panel of derivatives was applied to AgOr65 + AgOrco cells, they were, once again, all capable of blocking odorant-evoked currents at varying potencies (Figure 3). The AgOr65 complex displayed a similar potency sequence of HMA > MIA > DCBA ~ EIPA > Phenamil > DMA > Amiloride (see online supplementary Table S1 for IC$_{50}$ values). Interestingly, 1 amiloride derivative, DMA, was significantly less potent (*P* < 0.001) against the AgOr65 complex (IC$_{50}$ = −3.79±0.03 logM) compared with AgOr48 (IC$_{50}$ = −4.61±0.05 logM), suggesting that the odorant-specific tuning OR contributes to the site of DMA blockade.

We next examined whether amiloride derivatives could block insect OR currents when elicited by the Orco agonist, VUAA1 (Jones et al. 2011). Here, the most robust blockers from the odorant studies, HMA and MIA, also caused a concentration-dependent reduction in the VUAA1-induced currents of HEK cells expressing AgOrco together with either AgOr48 or AgOr65 (Figures 4 and online supplementary Figure S2). The IC$_{50}$ values for HMA (−5.41±0.04 logM) and MIA (−5.40±0.04 logM) against the AgOr48 complex were very similar to each other, which was also observed when agonized by δ-decalactone. Cells expressing AgOr65 + AgOrco displayed significantly higher sensitivity (*P* < 0.001) to HMA (−5.68±0.03 logM) than MIA (−5.38±0.06 logM), a

difference that was also observed in the eugenol studies. Both AgOr complexes were more susceptible to blockade when activated by VUAA1, suggesting that the VUAA1-bound channel is more accessible to HMA and MIA (see online supplementary Table S1). Again, the effects of blockade appeared to be slightly irreversible and independent of prolonged VUAA1 stimulation (see online supplementary Figure S1). These results demonstrate that amiloride derivatives are capable of blocking heteromeric AgOr complexes gated by VUAA1.

To determine if amiloride derivatives could also block homomeric Orco channels, we applied HMA and MIA to cells expressing AgOrco alone. Here, homomeric AgOrco channels were considerably more sensitive to HMA and MIA than any of the heteromeric AgOr complexes, with IC$_{50}$ values of −5.86±0.02 logM and −5.72±0.04 logM, respectively (Figures 5A and see online supplementary Figure S2C-D). In addition, we explored the effect of HMA on homomeric Orco channels from 3 different insect orders—*Harpegnathos saltator* (Hymenoptera, HsOrco), *Heliothis virescens* (Lepidoptera, HvOrco), and *Lygus hesperus* (Hemiptera, LhOrco)—to assess whether amiloride blockade was specific to AgOrs (Zhou et al. 2012; Wang et al. 2011; Hull et al. 2012). In these studies, VUAA1-evoked currents from each Orco ortholog were reduced with increasing concentrations of HMA, (Figures 5B–D). Moreover, HsOrco displayed the greatest sensitivity to HMA (−6.07±0.04 logM), whereas LhOrco was the least
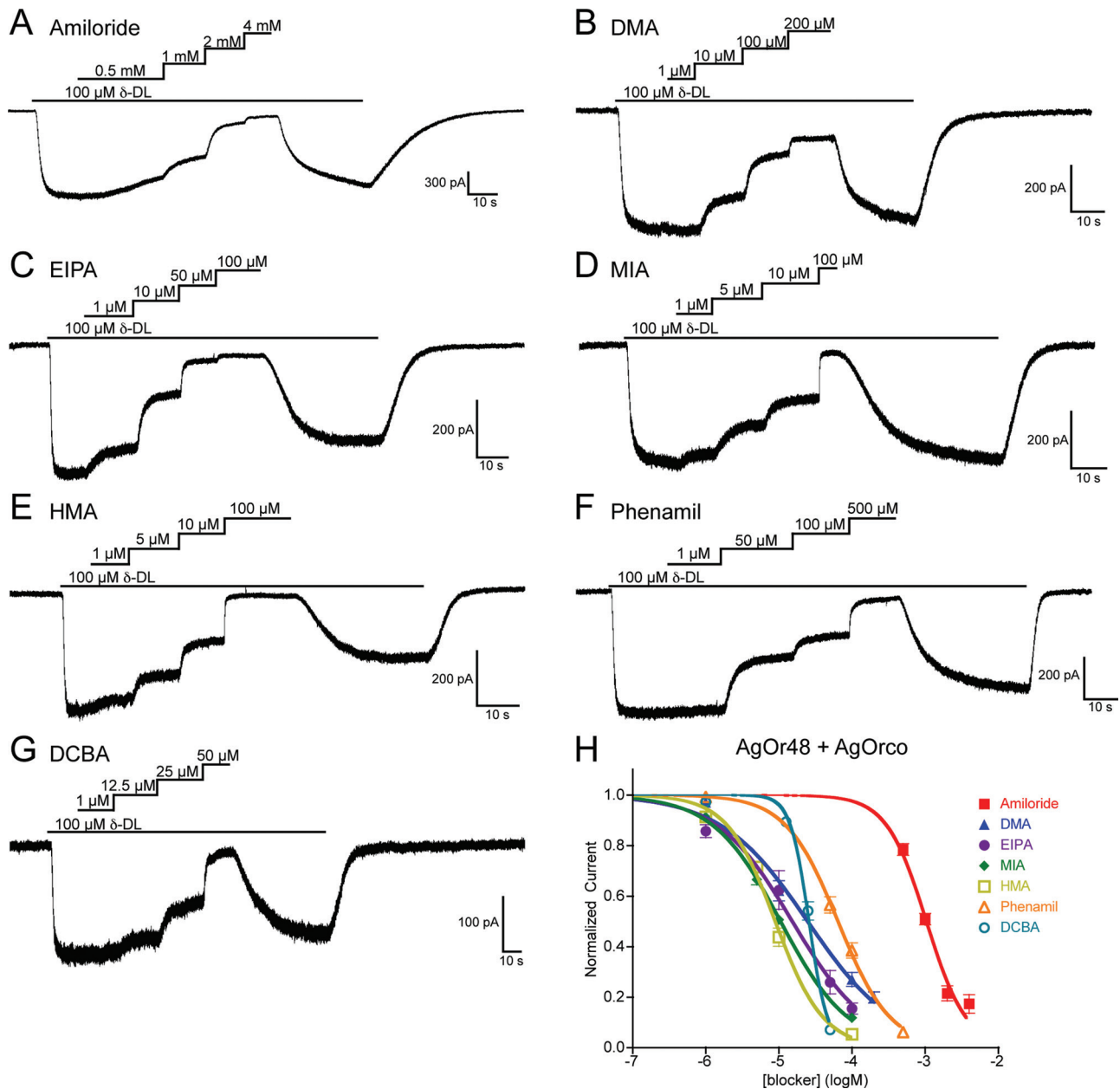
Figure 2 Amiloride derivatives block odorant-evoked whole-cell currents in AgOr48 + AgOrco cells. **(A–G)** Representative whole-cell recordings of HEK cells expressing AgOr48 + AgOrco. Cells were first stimulated by 100 μM δ-decalactone and then simultaneously subjected to increasing concentrations of the indicated amiloride derivative. Holding potentials ranged from −60 to −50 mV, and the solutions were Extracellular 1 and Internal 1. **(H)** Inhibition curves for each of the amiloride derivatives, with data points representing the normalized mean ± standard error mean (SEM) of the current reduction. IC$_{50}$ values and the number of trials (*n*) can be found in online supplementary Table S1.

sensitive to current blockade (−5.62 ± 0.04, Figure 5E). These results indicate that amiloride derivatives possess a broad ability to block Orco-containing complexes and can therefore be utilized to explore OR channel function across several insect taxa.

We next investigated the kinetics of the current inhibition on AgOr complexes by applying a high concentration of HMA (100 μM) to steady-state currents evoked by either VUAA1 or odorant. When applied, HMA exhibited significantly different inhibition kinetics (as defined as the time required to transition from 90% to 10% steady-state current amplitudes) across several of the AgOr complexes (Figure 6A–E). By this measure, VUAA1-induced currents in AgOrco cells displayed the most rapid current inhibition with an inhibition time of 319.4 ± 97.4 ms (Figure 6F).

To explore the mechanism of current block, we next examined whether HMA could bind AgOr complexes in the absence of agonist. The assay design consisted of 3 recording sweeps each containing an application of agonist,
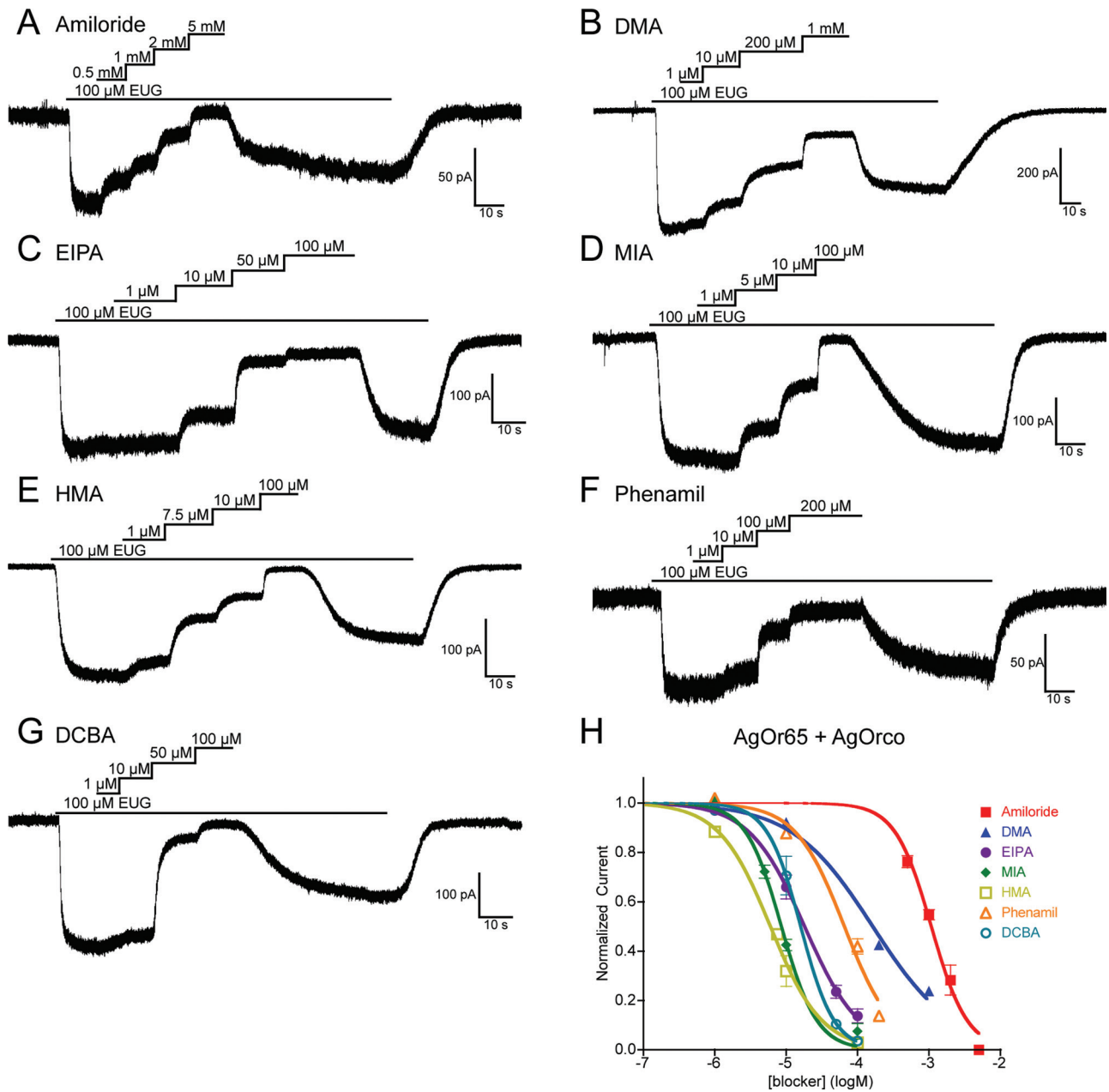
Figure 3 Odorant-evoked currents of the AgOr65 complex can be blocked by amiloride derivatives. **(A–G)** Representative whole-cell recordings of HEK cells expressing AgOr65 + AgOrco. After initial steady-state responses to 100 μM eugenol, increasing concentrations of the amiloride derivative were applied to each preparation. Holding potentials ranged from –60 to –50 mV, and the solutions were Extracellular 1 and Internal 1. **(H)** Inhibition curves for each of the amiloride derivatives, with data points representing the normalized mean ± SEM of the current reduction. IC_{50} values and the number of trials (*n*) are in online supplementary Table S1. A color version of this figure appears in the online issue of *Chemical Senses*.

with 100 μM HMA applied and washed out in Sweep 3 just before the third agonist stimulation (Figure 7A). With Sweep 1 serving as a normalization factor, potential differences in activation kinetics and current amplitude between Sweeps 2 and 3 can be compared to determine if the pre-application of HMA had an effect. In all instances, pre-exposure to HMA significantly reduced both the activation rate and current amplitude during Sweep 3, demonstrating that HMA can bind the AgOr complex in the absence of agonist

(Figure 7B–H). Furthermore, during the pre-agonist HMA application to AgOr48 + AgOrco-expressing cells, there was a consistent upward deflection in the baseline current that was not observed with either AgOr65 + AgOrco or AgOrco cells (see online supplementary Figure S3). This observation provides evidence that HMA can bind to and block the spontaneous opening currents of the AgOr48 complex and suggests that this complex has a higher rate of spontaneous opening than other AgOr complexes.
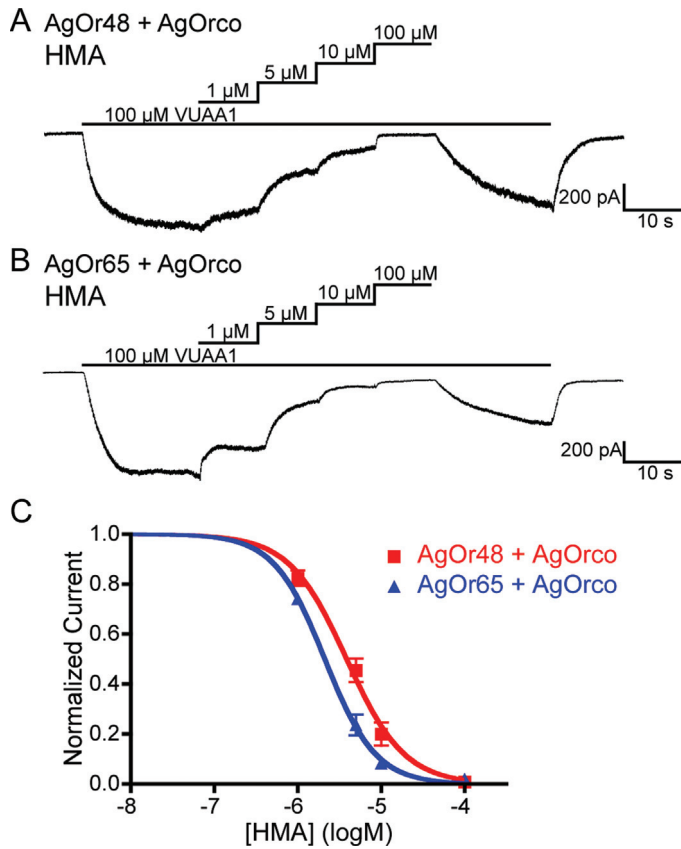
Figure 4 VUAA1-evoked currents are blocked by HMA. **(A–B)** Representative current traces from either AgOr48 or AgOr65 cells during stimulation with 100 μM VUAA1. Increasing amounts of HMA resulted in a reduction of VUAA1-evoked current that was partially irreversible after amiloride wash-out. The holding potential for each recording is −60 mV, and the solutions were Extracellular 2 and Internal 2. **(C)** Inhibition curves for HMA for each complex, with data points representing the normalized mean ± SEM of the current reduction. IC_{50} values and the number of trials (*n*) can be found in online supplementary Table S1. A color version of this figure appears in the online issue of *Chemical Senses*.
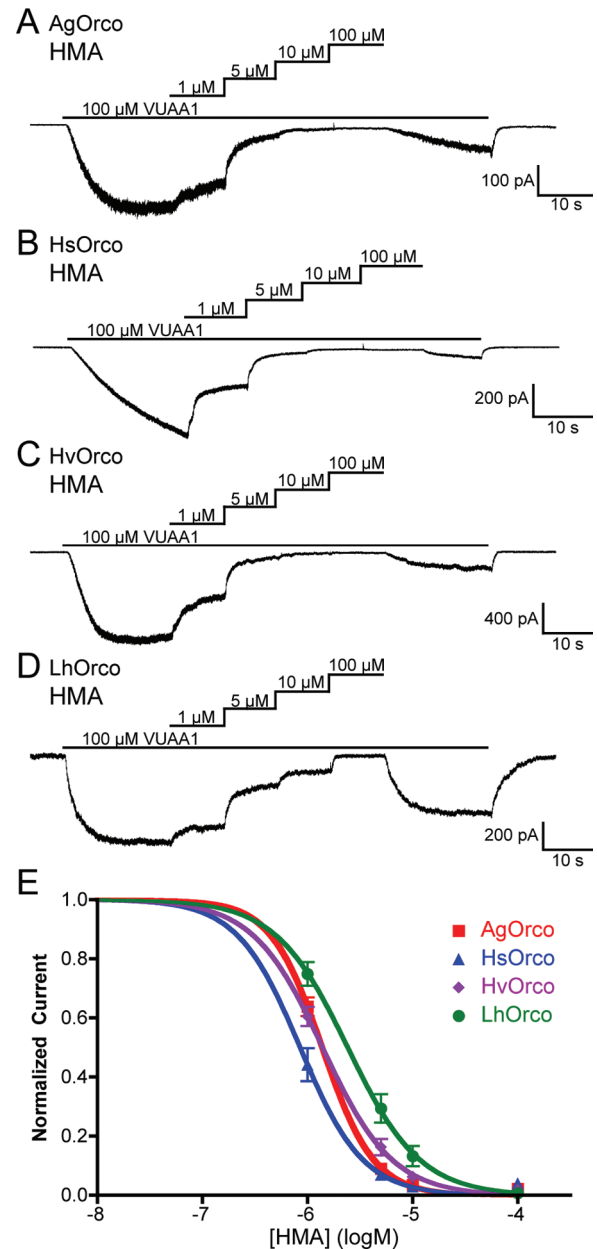
Figure 5 HMA also blocks homomeric Orco channels from four insect species. **(A–D)** Whole-cell responses from cells expressing Orco channels from *Anopheles gambiae* (**A, AgOrco**), *Harpegnathos saltator* (**B, HsOrco**), *Heliothis virescens* (**C, HvOrco**), or *Lygus hesperus* (**D, LhOrco**) to an application of 100 μM VUAA1. HMA reduced VUAA1-mediated currents in a concentration-dependent manner. The holding potential for each recording was −60 mV, and the solutions were Extracellular 2 and Internal 2. **(E)** Inhibition curves for HMA and MIA against AgOrco or HsOrco, with data points representing the normalized mean ± SEM of the current reduction. IC_{50} values and the number of trials (*n*) can be found in online supplementary Table S1. A color version of this figure appears in the online issue of *Chemical Senses*.

Discussion

This study identifies several amiloride derivatives that are capable of blocking insect OR ion channels when activated by an odorant ligand. The most potent blockers were HMA and MIA, and these derivatives were also able to block both heteromeric and homomeric currents during VUAA1 activation. Although the OR amiloride-binding domain remains uncharacterized, these data suggest that this site retains its susceptibility to amiloride derivatives, independent of the type of OR agonist or the tuning OR subunits present in the channel complex.

Though all of the OR complexes tested were susceptible to amiloride blockade, significant differences in sensitivity to the different analogs were observed. Indeed, the potencies of 3 amiloride derivatives were found to vary significantly between AgOr48 and AgOr65, the greatest of which was DMA, with nearly an order of magnitude difference in the IC_{50} values. Assuming that the site of amiloride blockade is within the OR channel pore as it is in ENaC, these data are in agreement with previous findings that the odorant-specific OR makes a significant contribution to the pore domain (Kelly et al. 2003; Nichols et al. 2011; Pask et al. 2011; Nakagawa et al. 2012).
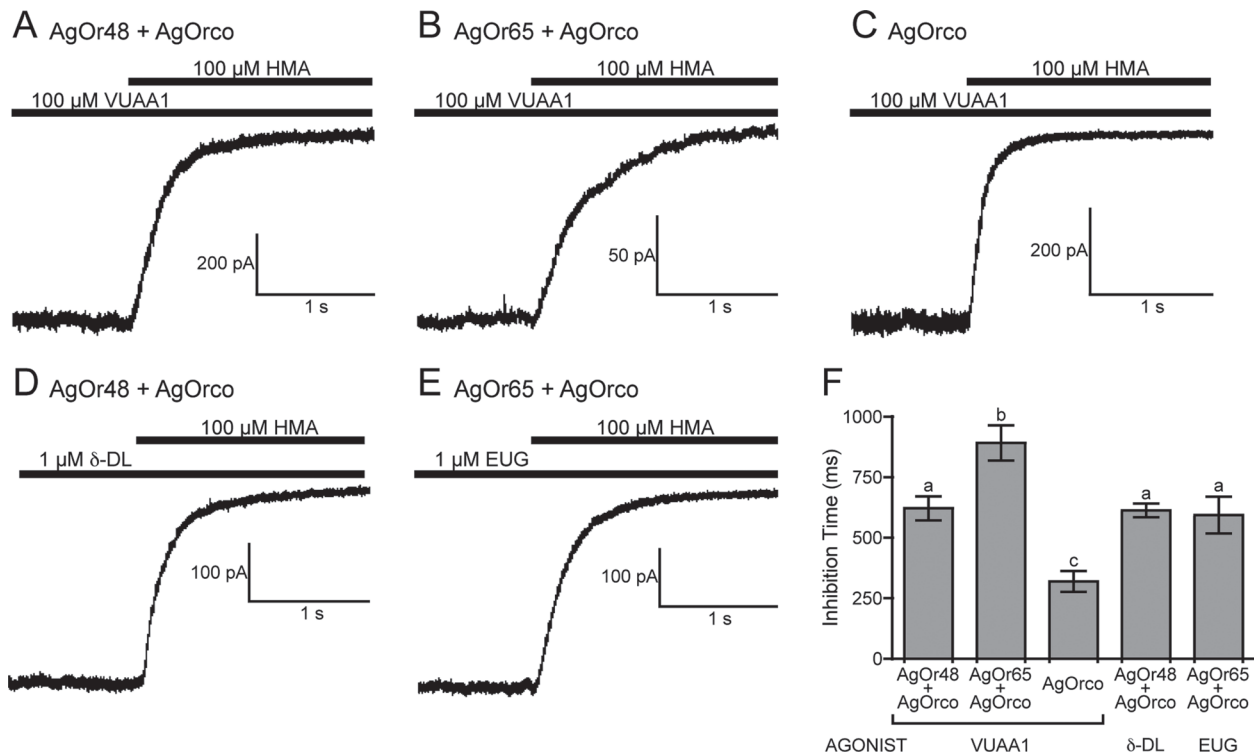
Figure 6 The rate of current inhibition by HMA varies among AgOr complexes. (**A-E**) Representative whole-cell currents of steady-state activation by either VUAA1 (100 μM) or odorant (1 μM) that were subsequently blocked by application of 100 μM HMA. (**F**) Histogram of the inactivation time (mean ± SEM, $n = 5$), or the time required to reduce the steady-state current from 90% maximal current to 10%, of the AgOr complexes. The holding potential for each recording was –60 mV, and the solutions were Extracellular 2 and Internal 2. Statistically different groups determined by an ANOVA and a Bonferroni post test ($P < 0.05$) are denoted by a, b, and c.

Interestingly, both the AgOr48 and AgOr65 cell lines were more susceptible to HMA and MIA blockade when activated by VUAA1 compared with gating by an odorant molecule. This effect could be due to the presence of functional homomeric Orco channels in the heteromeric AgOr cell lines or could suggest that the VUAA1-bound open state is more susceptible to amiloride blockade than the odorant-gated state. Homomeric AgOrco currents were more sensitive to HMA blockade than the heteromeric AgOr complexes, suggesting that the lack of an odorant-binding OR subunit results in a unique pore structure that is more sensitive to amilorides. These observations support the current model in which each insect OR complex exhibits a diverse channel pore, with significant contributions from both the Orco coreceptor and the odorant-sensitive OR (Nichols et al. 2011; Pask et al. 2011; Nakagawa et al. 2012). Moreover, the differences in HMA susceptibility among Orco orthologs suggest that, despite the high conservation of this protein across insect taxa, the nonconserved residues give rise to observable functional differences.

Although the precise mechanism of insect OR channel block by amiloride derivatives is still unknown, it appears that HMA is capable of binding and blocking ORs in the absence of agonist. In light of the well-established spontaneous opening of OR complexes, it cannot be determined whether HMA can bind to any channel state or only to the open channel (Sato et al. 2008; Jones et al. 2011). We believe the reduction of baseline current upon HMA application observed in AgOr48 + AgOrco cells reflects a higher spontaneous opening probability for AgOr48 + AgOrco complexes than either AgOr65 + AgOrco and AgOrco channels. It is reasonable to assume these OR-specific channel properties underlie the differences in spontaneous spike frequency previously observed in *Drosophila* ORNs in both endogenous neurons and the empty neuron (Hallem et al. 2004)

These studies demonstrate that amiloride derivatives can serve as potent pharmacological blockers of OR channels across 4 insect orders and can likely facilitate future mechanistic studies of these complexes, whether carried out in heterologous or *in vivo* systems. Furthermore, although both amilorides and ruthenium red have the ability to block many other types of ion channels, the large library of amiloride analogs may ultimately foster the identification of more specific blockers of insect ORs. Along with other molecular and pharmacological tools, the utilization of amiloride derivatives can lead to a greater understanding of the complex mechanisms involved in OR-based signal transduction
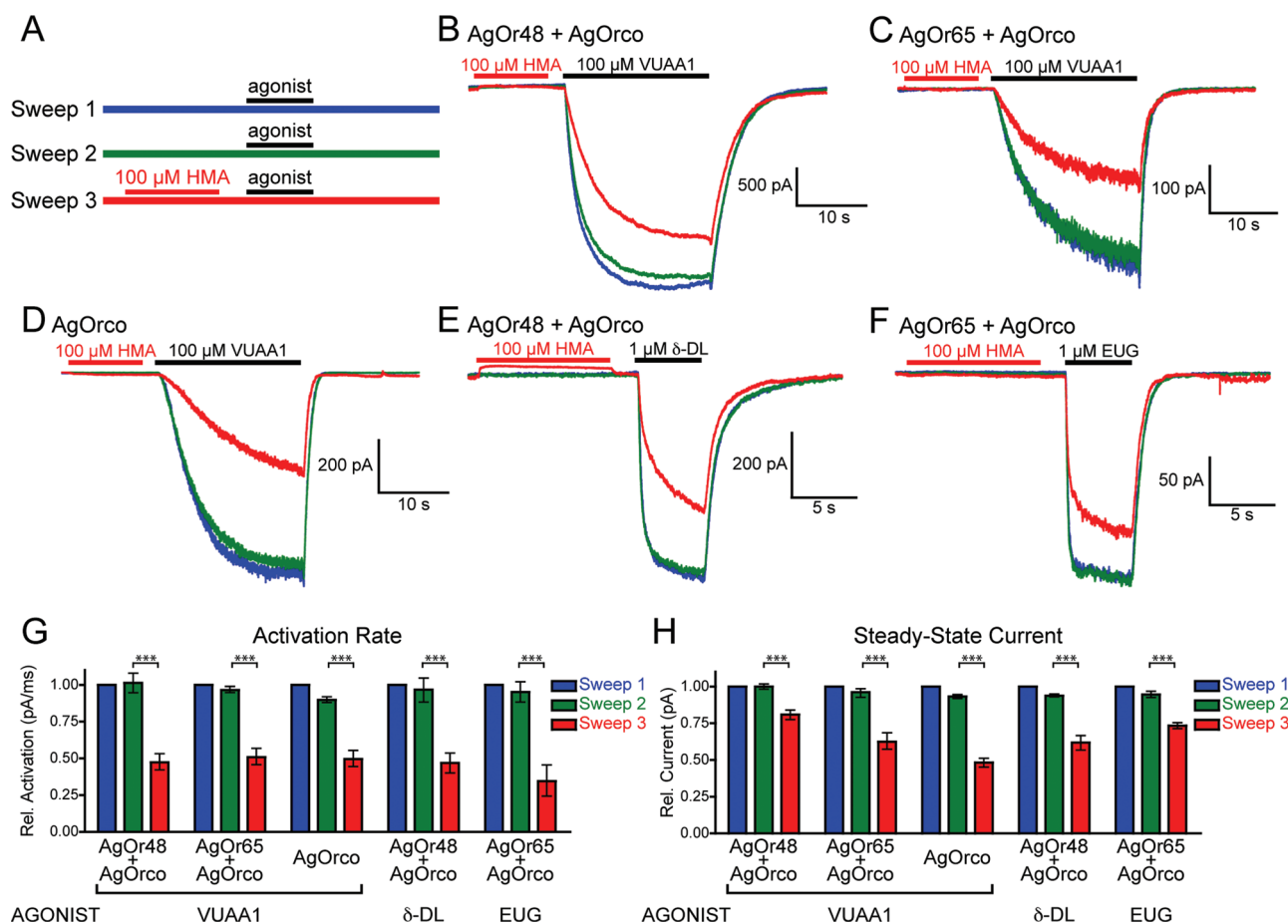
Figure 7 HMA can bind AgOr complexes in the absence of agonist. (**A**) Schematic of the assay consisting of 3 recording sweeps each containing a stimulation of agonist. Before the agonist application in Sweep 3, a 10 s pulse of HMA (100 μM) was applied to the cell. (**B–F**) Whole-cell recordings on several AgOr complexes as described in Figure 7A. The holding potential for each recording was −60 mV, and the solutions were Extracellular 2 and Internal 2. The effect of HMA on AgOr48 + AgOrco baseline currents is further examined in online supplementary Figure S3. (**G–H**) Histograms of both the activation rate from 10% to 90% maximal current (**G**) and the steady-state current (**H**) for each sweep ($n = 5$). The values for Sweeps 2 and 3 are normalized to Sweep 1 and compared with an ANOVA and Bonferroni post test (*** = $P < 0.001$). A color version of this figure appears in the online issue of *Chemical Senses*.

in insects. This may ultimately lead to the development of novel approaches to modulate critical olfactory behaviors in agricultural pests, disease vectors and other insects of global importance.

Supplementary material

Supplementary material can be found at http://www.chemse.oxfordjournals.org/

Acknowledgments

Funding

References

Abuin L, Bargeton B, Ulbrich MH, Isacoff EY, Kellenberger S, Benton R. 2011. Functional architecture of olfactory ionotropic glutamate receptors. Neuron. 69(1):44–60.

Benton R, Sachse S, Michnick SW, Vosshall LB. 2006. Atypical membrane topology and heteromeric function of Drosophila odorant receptors in vivo. PLoS Biol. 4(2):e20.

Bobkov YV, Ache BW. 2007. Block by amiloride derivatives of odor-evoked discharge in lobster olfactory receptor neurons through action on a presumptive TRP channel. Chem Senses. 32(2):149–159.

Bohbot JD, Jones PL, Wang G, Pitts RJ, Pask GM, Zwiebel LJ. 2011. Conservation of indole responsive odorant receptors in mosquitoes reveals an ancient olfactory trait. Chem Senses. 36(2):149–160.

Chen S, Luetje CW. 2012. Identification of new agonists and antagonists of the insect odorant receptor co-receptor subunit. PLoS ONE. 7(5):e36784.

Frings S, Lynch JW, Lindemann B. 1992. Properties of cyclic nucleotide-gated channels mediating olfactory transduction. Activation, selectivity, and blockage. J Gen Physiol. 100(1):45–67.

Hallem EA, Ho MG, Carlson JR. 2004. The molecular basis of odor coding in the Drosophila antenna. Cell. 117(7):965–979.

Hull JJ, Hoffmann EJ, Perera OP, Snodgrass GL. 2012. Identification of the western tarnished plant bug (*Lygus Hesperus*) olfactory co-receptor Orco: expression profile and confirmation of atypical membrane topology. Arch Insect Biochem Physiol. 81(4):179–198.

Jones PL, Pask GM, Rinker DC, Zwiebel LJ. 2011. Functional agonism of insect odorant receptor ion channels. Proc Natl Acad Sci USA. 108(21):8821–8825.

Jones PL, Pask GM, Romaine IM, Taylor RW, Reid PR, Waterson AG, Sulikowski GA, Zwiebel LJ. 2012. Allosteric antagonism of insect odorant receptor ion channels. PLoS ONE. 7(1):e30304.

Kaupp UB. 2010. Olfactory signalling in vertebrates and insects: differences and commonalities. Nat Rev Neurosci. 11(3):188–200.

Kelly O, Lin C, Ramkumar M, Saxena NC, Kleyman TR, Eaton DC. 2003. Characterization of an amiloride binding region in the alpha-subunit of ENaC. Am J Physiol Renal Physiol. 285(6):F1279–F1290.

Kleyman TR, Cragoe EJ Jr. 1988. Amiloride and its analogs as tools in the study of ion transport. J Membr Biol. 105(1):1–21.

Lundin C, Käll L, Kreher SA, Kapp K, Sonnhammer EL, Carlson JR, Heijne Gv, Nilsson I. 2007. Membrane topology of the Drosophila OR83b odorant receptor. FEBS Lett. 581(29):5601–5604.

Nakagawa T, Pellegrino M, Sato K, Vosshall LB, Touhara K. 2012. Amino acid residues contributing to function of the heteromeric insect olfactory receptor complex. PLoS ONE. 7(3):e32372.

Nakagawa T, Sakurai T, Nishioka T, Touhara K. 2005. Insect sex-pheromone signals mediated by specific combinations of olfactory receptors. Science. 307(5715):1638–1642.

Nichols AS, Chen S, Luetje CW. 2011. Subunit contributions to insect olfactory receptor function: channel block and odorant recognition. Chem Senses. 36(9):781–790.

Pask GM, Jones PL, Rützler M, Rinker DC, Zwiebel LJ. 2011. Heteromeric Anopheline odorant receptors exhibit distinct channel properties. PLoS ONE. 6(12):e28774.

Pask GM, Romaine IM, Zwiebel LJ. 2013. The molecular receptive range of a lactone receptor in Anopheles gambiae. Chem Senses. 38(1):19–25.

Sato K, Pellegrino M, Nakagawa T, Nakagawa T, Vosshall LB, Touhara K. 2008. Insect olfactory receptors are heteromeric ligand-gated ion channels. Nature. 452(7190):1002–1006.

Smart R, Kiely A, Beale M, Vargas E, Carraher C, Kralicek AV, Christie DL, Chen C, Newcomb RD, Warr CG. 2008. Drosophila odorant receptors are novel seven transmembrane domain proteins that can signal independently of heterotrimeric G proteins. Insect Biochem Mol Biol. 38(8):770–780.

Ugawa S, Ueda T, Ishida Y, Nishigaki M, Shibata Y, Shimada S. 2002. Amiloride-blockable acid-sensing ion channels are leading acid sensors expressed in human nociceptors. J Clin Invest. 110(8):1185–1190.

Wang G, Carey AF, Carlson JR, Zwiebel LJ. 2010. Molecular basis of odor coding in the malaria vector mosquito Anopheles gambiae. Proc Natl Acad Sci USA. 107(9):4418–4423.

Wang G, Vásquez GM, Schal C, Zwiebel LJ, Gould F. 2011. Functional characterization of pheromone receptors in the tobacco budworm Heliothis virescens. Insect Mol Biol. 20:125–133.

Wicher D, Schäfer R, Bauernfeind R, Stensmyr MC, Heller R, Heinemann SH, Hansson BS. 2008. Drosophila odorant receptors are both ligand-gated and cyclic-nucleotide-activated cation channels. Nature. 452(7190):1007–1011.

Zhou X, Slone JD, Rokas A, Berger SL, Liebig J, Ray A, Reinberg D, Zwiebel LJ. 2012. Phylogenetic and transcriptomic analysis of chemosensory receptors in a pair of divergent ant species reveals sex-specific signatures of odor coding. PLoS Genet. 8:e1002930.